Journal of Bioenergetics and Biomembranes, Vol. 12, Nos. 3/4, 1980

The Entry Process as the Target for Energy Input in Active Transport of α-Aminoisobutyric Acid by *Mycobacterium phlei*

R. Devés and A. F. Brodie

Department of Biochemistry
University of Southern California
School of Medicine
Los Angeles, California 90033

Received February 4, 1980; revised March 17, 1980

Abstract

Mycobacterium phlei was shown to accumulate α-aminoisobutyric acid, establishing a concentration gradient of approximately 15,000-fold. The apparent affinity constant of the carrier for α-aminoisobutyric acid was 1.8 μM. The system exhibited a broad specificity provided two structural requirements were satisfied: the presence of a free amino and carboxyl group on the alpha carbon and the absence of a net charge. The role of energy coupling on the accumulation of α-aminoisobutyric acid was studied by two different kinds of experiments, the relative effects of the inhibitors on the rate of entry and the steady-state of accumulation, and a comparison of the efflux induced at the final steady state by the addition of (a) excess nonradioactive α-aminoisobutyric acid, (b) energy inhibitors, or (c) both. The results are consistent with the hypothesis that accumulation of α-aminoisobutyric acid is due to an increased rate of entry, the rate of exit not being affected by metabolic inhibitors.

Introduction

It is well known that bacterial cells are capable of specifically transporting and accumulating amino acids. The maintenance of high concentration gradients, often several thousand times, requires the utilization of metabolic energy stored in the cell in the form of ionic gradients [1]. Numerous studies have been undertaken in an attempt to understand the special features of the transport process regarding its specificity, definite kinetic behavior, and the topology and structural characterization of its components [2]. In addition, intense research has been dedicated to investigate the nature of the energy source that supports this activity [3]. Comparatively little effort, however,

0145-479X/80/0800-0175$03.00/0

has been devoted to the very intriguing problem as to how information is transferred from an ionic gradient to the transporter.

Assuming that the same molecular entity is responsible for both the entry and exit of substrate, the magnitude of the concentration gradient at the final steady state (α) is determined by four experimental parameters: the maximum rates of entry ($\overline{V}_{So}$) and exit ($\overline{V}_{Si}$) and the half-saturation constants on the outer ($\overline{K}_{So}$) and inner ($\overline{K}_{Si}$) membrane face, according to the following expression (see Appendix):

$$\alpha = \left(\frac{[S_i]}{[S_o]}\right)_{final} = \frac{\overline{V}_{So}\overline{K}_{Si}}{\overline{V}_{Si}\overline{K}_{So}} \quad (1)$$

where $[S_i]$ and $[S_o]$ represent the concentration of substrate at the final steady state inside and outside the cell, respectively. It follows that the degree of accumulation will depend on an asymmetry imposed on one or more of these constants. In more general terms we can visualize the energy as affecting the final steady state either by increasing the rate of entry or decreasing the rate of exit defined by the pairs of constants $\overline{V}_{So}$, $\overline{K}_{So}$ and $\overline{V}_{Si}$, $\overline{K}_{Si}$ respectively, or by modifying both.

The present study was undertaken to determine the role of energy coupling in the transport of α-aminoisobutyric acid (AIB)[1] in *M. phlei*. The method used is simple and direct. It involves a comparison of the effects of unlabeled substrates and metabolic inhibitors when added to the external medium after the final steady state has been reached. The results demonstrate that the target for energy input is the entry process, the exit process remaining unaffected by de-energization.

Materials and Methods

Preparation of Cells

M. phlei ATCC 354 cells were grown as previously described [4] in a medium containing 0.2% Tween-80 as carbon source and devoid of Casamino acids. The cells were washed three times with 50 mM *N*-2-hydroxyethyl piperazine-*N'*-2-ethanesulfonic acid (Hepes-KOH), pH 7.45, containing 0.2% Tween-80 (4°C) and were resuspended in the same buffer to a protein concentration of approximately 10 mg/ml.

Transport Assay

Washed cells were preincubated (0.2–1.0 mg protein/ml) for 5 min at 30°C in a medium containing 45 mM Hepes-KOH buffer (pH 7.45) and

[1]The abbreviations used are: AIB, α-aminoisobutyric acid; Hepes, 4-(2-hydroxyethyl)-1-piperazineethanesulfonic acid; CCCP, *m*-chlorocarbonylcyanide phenylhydrazone; DNP, 2,4-dinitrophenol.

0.18% Tween-80 and the reaction was started by the addition of the desired concentration of [1-^{14}C] AIB.

a. Determination of the Radioactivity in the Cells. At indicated time intervals, 0.1 ml aliquots of cell suspension were removed and immediately diluted in 2.0 ml of chilled Hepes-KOH buffer (50 mM, pH 7.45). The suspension was rapidly filtered on 0.45 μm membrane filters (Millipore Corp.) and the cells washed twice with 2 ml of the same buffer. Dilution and filtration took less than 10 sec for completion. The radioactivity retained by the filters was determined with either a Nuclear-Chicago or a Beckman LS-8000 liquid scintillation detector, using 5 ml of Econofluor as scintillation solution.

b. Determination of the Radioactivity in the External Medium. Aliquots (0.1 ml) of the cell suspension were taken at different time intervals and immediately centrifuged in a Beckman Microfuge B for 1.5 min. The radioactivity present in the external medium was determined by counting an aliquot (25 or 50 μl) of the supernatant in 5 ml of Bray's solution with a Beckman LS-8000 liquid scintillation detector.

c. Total Radioactivity. The total radioactivity was routinely determined by counting a 0.05-ml aliquot of the cell suspension in 5 ml of Bray's solution.

Free Amino Acid Content of Whole Cells

Chromatography of boiled cell extracts was carried out in silica gel plates using three different solvent systems: (1) butanol:acetic acid:H_2O (4:1:1), (2) ethanol (95%):H_2O (7:3), and (3) phenol:H_2O (3:1). The chromatograms were developed by the use of a ninhydrin spray. When [1-^{14}C] AIB uptake was followed chromatographically, equal sections (1 cm) of the chromatograms were scrapped and the radioactivity in each section determined. Synthetic [1-^{14}C] AIB was used as standard. Solvents are given in volume ratios.

Hypoosmotic Shock

The effect of hypoosmotic shock on the intracellular amino acid pool was studied in two different ways.

a. Cells were incubated (0.5 mg protein/ml) in Hepes-KOH (45 mM, pH 7.45) and 0.18% Tween with [1-^{14}C] AIB (5.87 μM, specific activity 22.5 mCi/mmol) or [^{14}C(U)]-L-glutamic acid (25 μM, specific activity 20 mCi/mmol). After the final steady state was reached, the reaction mixture was made hypertonic by the addition of 0.1 volumes of 4 M NaCl. The osmolarity of the medium was 855 mOsm. Samples (0.1 ml) were then diluted in 2 ml of chilled Hepes-KOH (25 mM, pH 7.45, 34.5 mOsm) and the radioactivity in the cells was determined as described above.

b. A cell suspension (0.3–3 mg protein/ml) was made hypertonic by the addition of 0.4 M NaCl (855 mOsm). After 15 min of incubation an aliquot of the cell suspension (1 ml) was injected into 20 ml of ice cold Hepes-KOH (25 mM, pH 7.45, 34.5 mOsm) containing 0.18% Tween-80. The cells were centrifuged for 10 min at 7800 *g* and resuspended in 1 ml of hypertonic Hepes-KOH buffer; this procedure was repeated three times and the cells were then resuspended to a protein concentration of approximately 10 mg protein/ml. The percent amino acids retained was determined by three means: (1) a ninhydrin test in solution, (2) the inhibitory effect of a boiled extract on the entry rate of [1-^{14}C] AIB, and (3) the residual radioactivity when the cells had been preincubated with radioactive amino acids. Changes in the amino acid pool were also monitored by thin-layer chromatography.

Determination of Cell Water

Determination of intracellular volume commonly involves the use of radioactive inulin or dextran to estimate the proportion between extracellular and intracellular water. This method, however, could not be applied to *M. phlei* cells because their cell envelopes were found to interact strongly with both these polymers. Independent volume estimations were obtained by two different means.

a. The volume was determined from the microhematocrit and dry weight (2.29 mg dry weight/mg protein) of a dense suspension (20%) of known protein concentration. The percentage of packed cells was measured and the cell water calculated on the assumption that the extracellular volume in this pellet was 10% and the cell specific gravity was 1.1. The results obtained by this method and the determination of the inulin space, when compared by Winkler and Wilson [5], were shown to agree. The result from three experiments was found to be 5.88 ± 0.31 μl H_2O/mg protein.

b. A dense cell suspension (20%) of known protein concentration containing ^{3}H-H_2O (0.5 μC/ml) was centrifuged in a Beckman Microfuge B and the total water in the pellet determined from the ^{3}H-H_2O distribution. The intracellular H_2O volume, calculated on the assumption that 10% of the water in the pellet was extracellular water, was found to be 7.08 ± 0.02 μl H_2O/mg protein.

The average of these two values, 6.5 μl H_2O/mg protein, was used for the calculation of internal concentration.

Concentration of Intracellular Amino Acids

The relative concentration of the amino acid pool was determined with ninhydrin. The reagent was prepared by dissolving 0.4 g ninhydrin and 8 mg stannus chloride in 20 ml of acetate buffer (1 part of 4 M acetate, pH 5, 3 parts of ethylene glycol). The reaction was carried out by boiling 1 ml of

ninhydrin reagent and a sample of the cell extract (equivalent to 0.05–2 mg protein) for 10 min. Following dilution with 4 ml propanol:H_2O (1:1), the relative amino acid content of the extracts was estimated from the absorbance at 570 nm.

Composition of the Amino Acid Pool

Amino acid analysis of the boiled cell extract was performed on a Durrum Dionex D 500 amino acid analyzer [6].

Protein Determination

The cells were precipitated with 10% trichloroacetic acid and centrifuged at 2000 *g* for 5 min. The pellet was suspended in 1 N NaOH and heated at 90°C for 5 min to ensure solubilization. Protein was estimated by the method of Lowry et al. [7].

Results

Time Course of [1-^{14}C] AIB Uptake by M. phlei

M. phlei was shown to accumulate AIB, an analog of alanine, establishing a concentration gradient of approximately 15,000-fold. The time course of accumulation as well as the disappearance of label from the external medium are shown in Fig. 1. Chromatography of boiled extracts of these cells after 5, 20, and 40 min of incubation with [1-^{14}C] AIB showed no evidence of chemical modification of the amino acid analog. A Lineweaver–Burk plot of the initial rate of entry at different AIB concentrations revealed a K_m of 1.81 μM (correlation coefficient 0.985). The range of concentrations tested was from 0.485 to 9.7 μM.

Effects of Various Analogs on the Initial Rate of Entry of AIB

The relative apparent affinities for a number of amino acids with respect to AIB were determined by comparing the initial rate of entry of AIB in the presence and absence of the unlabeled amino acid by means of the following expression (see Appendix):

$$\frac{\overline{K}_{To}}{\overline{K}_{So}} = \frac{[T_o]/[S_o]}{(v_o/v - 1)(1 + \overline{K}_{So}/[S_o])} \tag{2}$$

$[S_o]$ and $[T_o]$ are the external concentrations of AIB and analog respectively, v and v_o are the initial rates of entry of AIB in the presence and absence of unlabeled amino acid respectively, and $\overline{K}_{To}/\overline{K}_{So}$ is the relative apparent affinity constant of the carrier for the analog with respect to that for AIB.

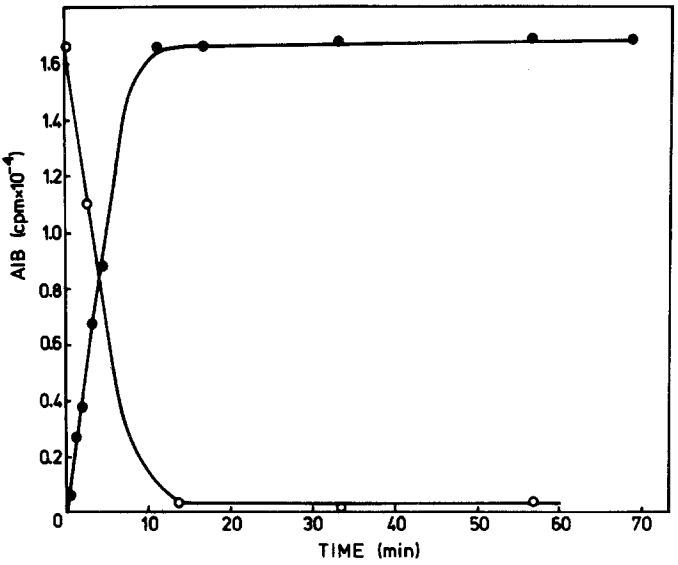

Fig. 1. Time course of AIB uptake in *M. phlei*. A cell suspension was incubated (1 mg protein/ml) in Hepes-KOH buffer (45 mM, pH 7.45) and 0.18% Tween-80 at 30°C. The total volume of the reaction mixture was 3 ml. Samples (0.1 ml) were withdrawn at indicated time intervals and the radioactivity in the cells or the external medium determined as described under Materials and Methods. The initial concentration of AIB in the external medium was 9.45 μM and the specific activity was 14.0 mCi/mmol ($1.8 \cdot 10^4$ cpm/nmol). The values plotted represent the radioactivity present in 0.1 ml of reaction mixture; (•) radioactivity in the cells; (○) radioactivity in the external medium. The uptake in the final steady state is equal to 9.3 nmol/mg protein.

Equation (2) involves the assumption that the mechanism is competitive. The term $(1 + \overline{K}_{So}/[S_o])$ in Eq. (2) was determined in each experiment from the inhibition observed in the presence of unlabeled AIB (16.2 μM), since under these conditions $\overline{K}_{To}/\overline{K}_{So}$ equals 1.0.

As shown in Table I, the carrier did not exhibit significant affinity for any of the charged amino acids tested (L-aspartic acid, L-glutamic acid, L-cystine, L-arginine). In addition, the low affinity of the carrier for proline and the di- and tripeptides including the small glycine-L-alanine dipeptide probably reflects the requirement for a proximal free amino and carboxyl group. On the other hand, provided these two requirements were satisfied, i.e., the absence of a net charge and the presence of a free amino and carboxyl group on the alpha carbon, the carrier exhibited a broad specificity and indeed significant interaction could be demonstrated for all the neutral amino acids tested with the exception of L-cystine. The lower limits given for the relative half-saturation constants in Table I were calculated on the basis that

Table I. Relative Half-Saturation Constants for Various Analogs with Respect to That for AIB

Analog	Relative concentration in the assay [analog]/[[1-^{14}C] AIB] = $[T_0]/[S_0]$	Relative half-saturation constant (analog with respect to AIB) $\bar{K}_{To}/\bar{K}_{So}$
L-α-Aminoisobutyric acid	1.62	1.00
L-Alanine	1.85	0.45
L-Serine	1.88	0.56
L-Tryptophan	1.65	0.62
L-Glycine	2.22	0.65
L-Valine	1.53	0.72
L-Leucine	1.58	0.73
L-Methionine	1.89	0.82
L-Phenylalanine	1.72	0.96
L-Glutamine	1.47, 3.12	1.12
L-Isoleucine	1.8	1.22
L-Tyrosine	1.62	1.35
L-Histidine	1.70	2.25
L-Asparagine	1.70	5.73
Glycyl-L-alanine	103.10	36
L-Leucyl-glycine	103.10	46
L-Glutamic acid	1.51, 93.1, 973.5	130
L-Aspartic acid	1.77	>13
L-Lysine	1.71	>13
L-Arginine	1.75	>13
L-Cystine	1.58	>13
Glycyl-L-alanyl-L-alanine	1.55, 15.5	>120
α-L-Glutamyl-L-leucine	1.55, 15.5	>120
L-Proline	1.5, 20	>150

a 10% difference in the rates of entry of AIB in the absence and presence of analog ($v_o/v = 1.11$) would have been experimentally significant.

It should be noted that L-phenylalanine at a concentration of 130 μM inhibits the rate of entry of 9.45 μM AIB by 92.6%, as predicted by the affinity constant calculated from Table I (1.7 μM). Partial inhibition would have been observed if AIB were entering through two separate routes that differed significantly in their affinity for L-phenylalanine, for example an alanine and a phenylalanine carrier.

Effect of the Analogs when present on the trans *Side of the Membrane with Respect to [1-^{14}C] α-Aminoisobutyric Acid*

Inhibition of the initial rate of entry could be simply the reflection of binding to the carrier at the external surface and does not in itself prove that the analog enters the cell through the inhibited path. Therefore the effect of the analogs when present on the *trans* side of the membrane with respect to

internal [1-^{14}C] AIB was investigated. The behavior expected under these experimental conditions is different whether the analog is transported or only binds from the external surface. If the analog present in the external medium is transported through the AIB carrier, net efflux of labeled AIB will be observed. The efflux results from an exchange between the unlabeled analog present outside and the [1-^{14}C] AIB inside the cell. Exit continues to occur while there is excess cold amino acid outside which can act as a sink for the exiting labeled material, and while the concentration of analog inside the cell is low enough not to compete with AIB for exit. If the analog, however, is not a substrate for the system, exchange will not be observed since the carrier will be held at the external surface.

M. phlei cells were incubated with [1-^{14}C] AIB and after the final steady state was reached, 1 mM unlabeled amino acid was added to the external medium and the appearance of radioactivity in the external medium was followed as described in Materials and Methods. The molar ratio of the unlabeled analog with respect to the [1-^{14}C] AIB in the external medium when the reaction was started was approximately 10^4.

The effect of AIB, L-phenylalanine, L-histidine, and L-tryptophan when present on the *trans* side with respect to internal [1-^{14}C] AIB is shown in Fig. 2. These particular amino acids were chosen because of their dissimilarity in structure with respect to AIB. The results show that the three amino acids tested are transported by the same system as AIB. Furthermore, under these experimental conditions efflux of [1-^{14}C] AIB is a direct reflection of the rate of entry of the unlabeled amino acid present in the external medium [8]. Therefore the identity in the rate of the induced exit indicates that all the amino acids tested enter the cell at the same rate. The rate of exit of the label

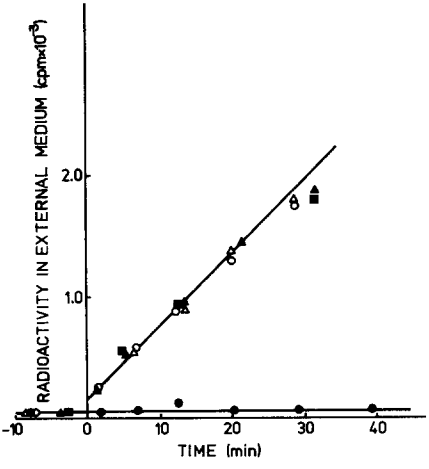

Fig. 2. Effect of AIB, L-phenylalanine, L-tryptophan, and L-histidine when present on the *trans* side of the membrane with respect to internal [1−^{14}C] AIB. Cells were incubated (1 mg protein/ml) with 9.7 μM [1−^{14}C] AIB (13.7 mCi/mmol, 2.2 · 10^4 cpm/nmol) at 30°. After the final steady state had been reached, unlabeled amino acid was added to the reaction mixture to a final concentration of 1 mM. Samples (0.1 ml) were taken at time intervals and the radioactivity in the supernatant determined as described under Materials and Methods. The values given represent the radioactivity in the external medium in 0.05 ml of reaction mixture. The time scale refers to the elapsed time following the addition of unlabeled amino acid. (○), AIB; (△), L-phenylalanine; (▲), L-tryptophan; (■), L-histidine; (●), no addition.

in Fig. 2 excluding the samples taken after 22 min is 55.2 cpm/mg protein · min (correlation coefficient 0.991).

Composition of the Amino Acid Pool in M. phlei

In spite of the fact that the cells are grown in the absence of amino acids, with Tween-80 as the only carbon source, chromatographic analysis of cell extracts revealed a significant amino acid pool. The possibility therefore had to be considered that the gradient observed was apparent and simply reflected an exchange between the [1-^{14}C] AIB and the amino acid pool.

A quantitative analysis of the amino acid content of the intracellular compartment carried out with an automated amino acid analyzer is shown in Table II. Attention should be drawn to the higher molar ratios of glutamic acid and glutamine with respect to the other amino acids in the pool. They constitute 80.35% and 14.7% of the pool respectively. The concentration of aspartic acid, threonine, and serine could not be estimated due to overlapping with the glutamate elution peak. It should also be noted that proline was not determined; other amino acids not listed in Table II were not present in detectable amounts.

When an aliquot (20 μl) of the boiled extract used for amino acid analysis (original cell suspension 21 mg protein/ml) was added to the reaction mixture, the initial rate of entry of [1-^{14}C] AIB was inhibited by 61.5%. This figure agrees well with the inhibition predicted from the amino

Table II. Composition of the Amino Acid Pool in *M. phlei*[a]

Amino acid	nmoles/mg protein	Concentration (mM)	Relative amount (%)	Equivalent AIB concentration (mM)
Glutamic acid	177.6	27.30	80.35	0.21
Glutamine	32.45	5.00	14.71	4.46
Alanine	3.65	0.56	1.65	1.37
Glycine	2.3	0.35	1.03	0.54
Lysine	1.66	0.26	0.76	—
Valine	1.11	0.17	0.50	0.24
Tyrosine	0.50	0.078	0.23	0.057
Leucine	0.47	0.072	0.21	0.1
Half cystine	0.29	0.045	0.13	—
Phenylalanine	0.19	0.029	0.09	0.03
Cystathione	0.21	0.032	0.09	—
Isoleucine	0.20	0.030	0.09	0.025
Arginine	0.15	0.023	0.07	—
Methionine	0.11	0.016	0.05	0.019
Histidine	0.069	0.011	0.03	0.026

[a]The concentration of the amino acids in the pool was calculated on the basis of an intracellular water volume of 6.5 μl/mg protein (see Materials and Methods). The last column shows the concentration of each amino acid divided by $\overline{K}_{To}/\overline{K}_{So}$ (the relative half-saturation constant for the analog with respect to that for AIB, Table I).

acid analysis and the relative half-saturation constants shown in Table I, which is 62.2%. If the assumption is made that the relative specificity of the carrier on the internal membrane surface is similar to that on the external surface, the amino acid pool would be equivalent to 6.37 mM AIB. The concentration of the pool, determined from its inhibitory effect on the rate of entry of AIB, in three other experiments with different cell extracts was shown to be equivalent to 5.98, 6.32, and 7.57 mM AIB.

Pool Removal by Osmotic Shock

The effect of hypoosmotic shock on cells preloaded with [1-^{14}C-AIB] and [^{14}C(U)] glutamate is shown in Fig. 3. The cells were incubated with radioactive amino acids and the reaction mixture was then made hypertonic by addition of NaCl. Samples were taken at time intervals, diluted in Hepes-KOH buffer (25 mM, pH 7.4), and filtered. The residual radioactivity was determined as described. A preincubation period of 8 min with NaCl was necessary for effective pool removal, presumably to allow the NaCl to enter into the cell.

A consistent difference was found in the sensitivity of the pool to osmotic shock depending on the method used to estimate the residual amino acids. Amino acids that had been recently accumulated were released easily; (95, 96, and 88% in the case of [1-^{14}C-AIB] and 83.6% for [^{14}C(U)] glutamate, after one shock). However, if disappearance of the pool was followed either by a ninhydrin test or its inhibitory effect on the initial rate of entry of [1-^{14}C] AIB, the percentage of amino acid removed by three consecutive shocks in six different experiments was only 32, 42, 50, 57, 60, and 62%. Chromatographic analysis of the cell extracts showed that the relative concentrations of the major components of the pool did not vary after three shocks. This difference

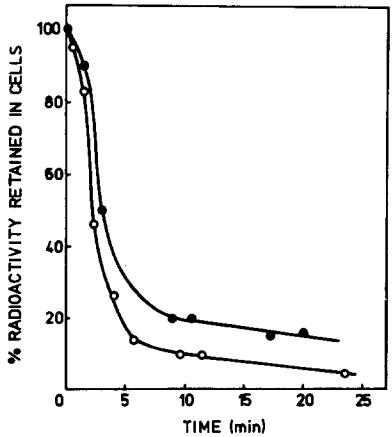

Fig. 3. Pool removal by osmotic shock. *M. phlei* cells were incubated (0.36 mg/ml) with 5.87 μM AIB (specific activity 22.47 mCi/mmol) or 25 μM L-glutamic acid (specific activity 20.0 mCi/mmol) as described for the transport assay. After the final steady state was reached, the suspension was made hypertonic (855 mOsm) by the addition of 0.1 volumes of 4 M NaCl. Samples were taken at time intervals into 2 ml Hepes-KOH buffer (25 mM, pH 7.45, 34.5 mOsm) and the residual radioactivity in the cells estimated as described under Materials and Methods. (○), [1−^{14}C] AIB; (●), [^{14}C(U)] glutamic acid.

suggests the existence of two different amino acid pools exhibiting different degrees of shock resistance.

Given the relatively high shock resistance of the amino acid pool, the effect of complete removal of the intracellular amino acids on the uptake of AIB could not be tested. It should be noted, however, that a 42% removal of the pool, as measured with ninhydrin, did not have any effect on the initial rate of entry of [1-^{14}C] AIB [control cells 0.68 nmoles/min · mg protein (correlation coefficient 0.999); shocked cells 0.69 nmoles/min · mg protein (correlation coefficient 0.999)], or a significant effect on the ability of the cells to accumulate AIB. Normal and shocked cells (1 mg/ml) were able to take up 98.8% and 97% of the radioactivity initially present in the external medium respectively.

Effect of Metabolic Inhibitors on the Rate of Entry

An important clue to the mechanism of energization came from the observation that metabolic inhibitors such as cyanide, 2,4-dinitrophenol (DNP), m-chlorocarbonylcyanide phenylhydrazone (CCCP), and arsenate drastically inhibited AIB uptake (Table III). If energization were affecting only the parameters for exit ($\overline{V}_{Si}$ $\overline{K}_{Si}$) without changing those for entry ($\overline{V}_{So}$, $\overline{K}_{So}$), complete inhibition of the AIB entry rate by metabolic inhibitors would have probably not been observed. Under these circumstances the amino acids in the pool would have been able to exchange with the [1-^{14}C] AIB in the external medium, giving rise to an apparent concentration of the label even in the absence of an energy source. This phenomenon has been demonstrated for the lactose carrier in *E. coli,* both in whole cells [9], and membrane vesicles [10]. De-energization therefore imposed a barrier before [1-^{14}C] AIB had a chance to enter into the cell. It should also be noted that cells (1 mg protein/ml) which were preincubated for 40 min as opposed to the usual 5 min, before addition of [1-^{14}C] AIB (25 μM), did not exhibit an inhibited rate of entry, indicating that the concentration of amino acid that leaked out in 40 min was negligible. The evidence presented above taken together with the fact

Table III. Effect of Metabolic Inhibitors on Active Transport of AIB[a]

Inhibitor	Concentration (mM)	% Inhibition of the entry rate
m-Chlorocarbonylcyanide phenylhydrazone	0.1	100
2,4-Dinitrophenol	5.0	93.6
Cyanide	10.9	95.7
Arsenate	50.0	90.6

[a]Entry rates were determined by incubating cells (0.3–0.5 mg/ml) with 9.7 μM AIB (14 mCi/mmol) as described under Materials and Methods. The inhibitors were added to the cell suspension 30 sec before the reaction was started.

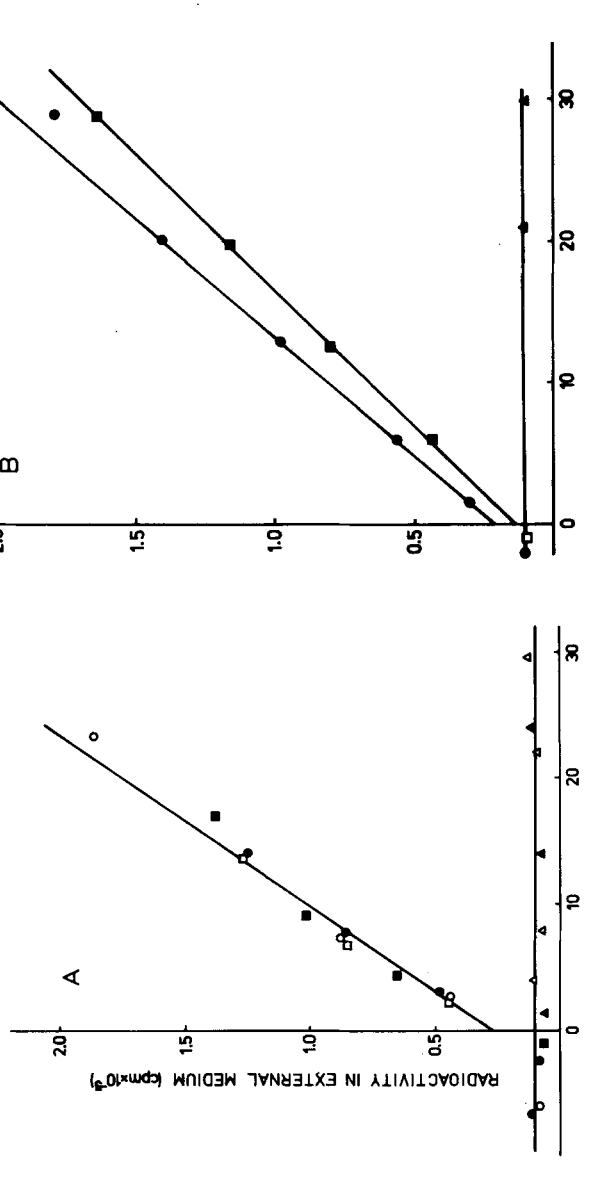

Fig. 4. Comparative effects of metabolic inhibitors and AIB when added at the final steady state to a cell suspension preincubated with [1—^{14}C] AIB. Cell suspensions were incubated with 9.7 μM [1—^{14}C] AIB (13.7 mCi/mmol, $2.2 \cdot 10^4$ cpm/nmol) at 30°C and after the final steady state had been reached, either a metabolic inhibitor or unlabeled AIB was added to the reaction mixture. Samples (0.1 ml) were taken at indicated time intervals and the appearance of radioactivity in the supernatant was followed as described under Materials and Methods. The values plotted correspond to the radioactivity present in 0.05 ml of external medium. The results of three experiments of this kind are shown here. The time scale refers to the elapsed time following the addition of AIB or metabolic inhibitor. (A) Experiment I: (○), 1 mM AIB; (□), 0.09 mM CCCP (4.75% ethanol); (△), no additions. Cell suspension: 0.6 mg protein/ml. Experiment II: (●), 1 mM AIB; (■), 10 mM DNP (4.75% ethanol); (▲), 4.75% ethanol. Cell suspension: 0.82 mg protein/ml. (B) Experiment III: (●), 1 mM AIB; (■), 8.4 mM KCN; (▲), no additions. Cell suspension: 1.4 mg protein/ml.

that the cells were grown in the absence of amino acids demonstrates that the cells were able to maintain an extremely high concentration gradient.

Comparative Effects of Metabolic Inhibitors and AIB when Added to a Cell Suspension Preincubated with [1-^{14}C] AIB

The role of energy coupling on the accumulation of AIB was further investigated by comparing the effects of unlabeled AIB and metabolic inhibitors, when added to a cell suspension preincubated with [1-^{14}C AIB]. The inhibitors were added at a concentration sufficient to produce virtually complete inhibition of the entry rate (Table III). As shown in Figs. 4A and 4B, unlabeled AIB (1 mM), DNP (10 mM), cyanide (10.9 mM), and CCCP (0.09 mM) had the same effect. The relative rates of the efflux induced by the inhibitors with respect to that induced by AIB for the experiments shown in Figs. 4A and 4B were found to be $v_{CCCP}/v_{AIB} = 1.04$, $v_{DNP}/v_{AIB} = 1.04$, and $v_{KCN}/v_{AIB} = 0.87$. Increasing the concentration of CCCP or cyanide by twofold did not affect the rate of exit of the label. Furthermore, the simultaneous addition of CCCP and AIB did not induce a greater efflux than the separate addition of either one. The rate obtained from a linear regression analysis of the pooled samples under these three conditions [AIB (1 mM); CCCP (0.09 mM); AIB (1 mM) and CCCP (0.09 mM)] was found to be 0.05 nmoles AIB/mg protein · min (correlation coefficient 0.994).

The coincidence in the rates of the efflux induced by AIB (exit process in the energized state) and the metabolic inhibitors (exit process in the de-energized state) strongly suggests that the exit process is not affected by energization.

Comparative Effects of Cyanide and CCCP on the Entry Rate and the Steady-State Level of Accumulation

Further evidence for the proposition that the entry step is the primary target for energy input was obtained from a comparison of the effects of different inhibitor concentrations on the entry rate (Figs. 5A, 5B) and on the steady-state level of accumulation (Figs. 6A, 6B). The effect of a given concentration of inhibitor on the steady state and the rate of entry was found to be of a comparable magnitude. For example, 25 μM CCCP inhibited the entry rate by 61% (Fig. 5B) and 23 μM reduced the concentration gradient by approximately 50% (Fig. 6B); this would not have been the case if the entry rate were not the primary target for energization. It should be noted that whereas in the case of cyanide the degree of inhibition of the rate of entry is a linear function of the inhibitor concentration (Fig. 5A), the dependence on the concentration of CCCP is of a higher order (Fig. 5B).

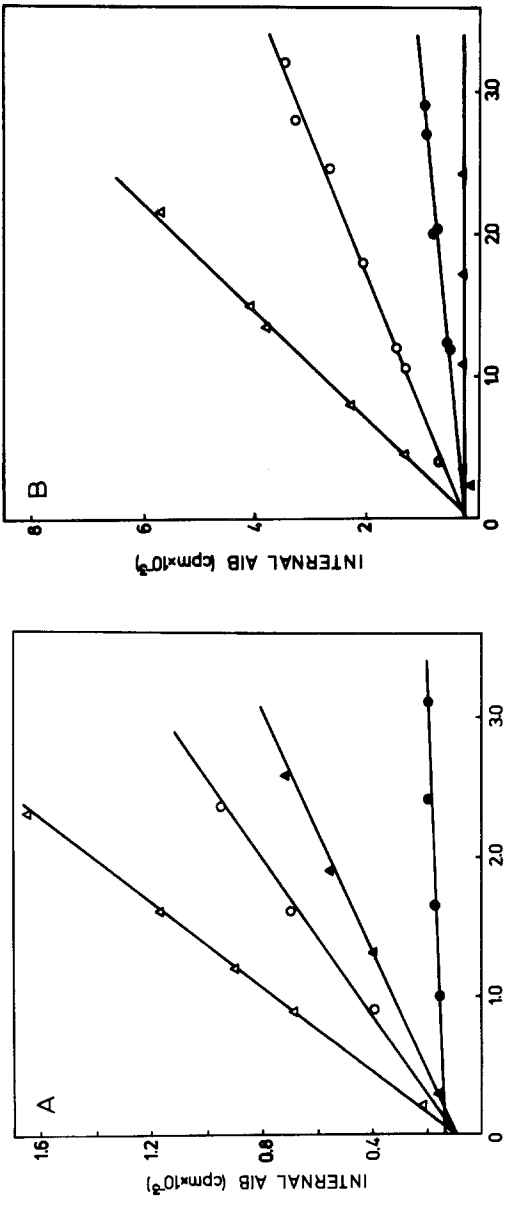

Fig. 5. Inhibition of the rate of entry by different concentrations of CCCP and KCN. Cells were incubated with 9.7 μM AIB (13.7 mCi/mmol, $2.2 \cdot 10^4$ cpm/nmol) at 30°C in the presence or absence of different concentrations of metabolic inhibitor. The inhibitor was added to the cell suspension 30 sec before the reaction was started. The entry rate was determined as described under Materials and Methods. (A) (△), no additions; (○), 0.54 mM KCN; (▲), 1.09 mM KCN; (●), 10.90 mM KCN. Cell suspension: 0.67 mg protein/ml. (B) (△), 4.75% ethanol; (○), 25 μM CCCP; (●), 50 μM CCCP; (▲) 100 μM CCCP. The ethanol concentration was the same in all assays (4.75%). Cell suspension: 0.5 mg protein/ml.

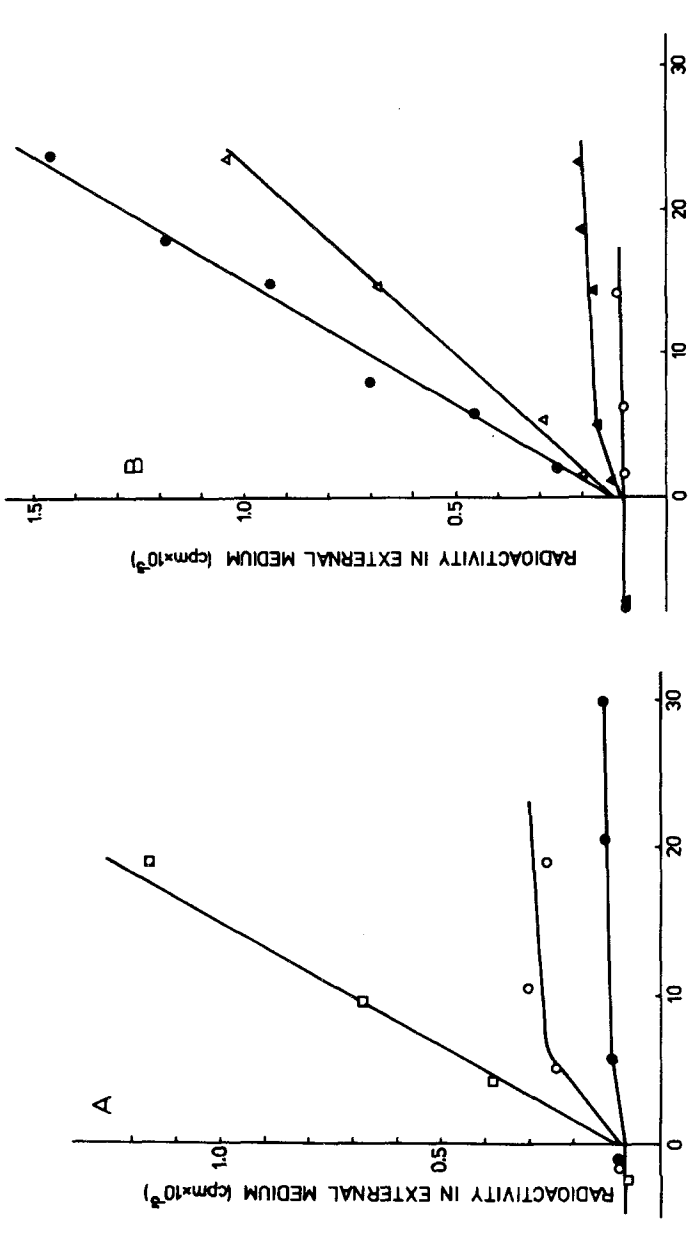

Fig. 6. Effect of different concentrations of KCN and CCCP on a cell suspension preincubated with [1-^{14}C] AIB. A cell suspension was incubated with 9.7 μM AIB (13.7 mCi/mmol, $2.2 \cdot 10^4$ cpm/nmol) at 30°C and after the final steady state was reached either KCN or CCCP was added to the reaction mixture. The appearance of radioactivity in the supernatant was followed as described under Materials and Methods. The time scale refers to the elapsed time following the addition of inhibitor. (A) (□), 10.9 mM KCN; (○), 2.1 mM KCN; (●), 0.54 mM KCN. Cell suspension: 1.34 mg protein/ml. (B) (●), 91 μM CCCP; (△), 46 μM CCCP; (▲), 23 μM CCCP; (○), 4.75% ethanol. The concentration of ethanol was the same in all assays (4.75%). Cell suspension: 1.0 mg protein/ml.

Discussion

The evidence presented in this paper strongly suggests that the energized step in the transport of neutral amino acids in *M. phlei* is the entry process. This was indicated in part by the comparative effects of metabolic inhibitors and unlabeled substrates added after the final steady state was achieved to a cell suspension that had been incubated with radioactive AIB (Figs. 4A, 4B). Both substrates and metabolic inhibitors perturb the system, but they do so by different means. Unlabeled substrates induce an efflux of the label by diluting the radioactive AIB in the external medium, initiating an exchange reaction between the internal label and the unlabeled substrate outside (Figs. 2, 4A, 4B). The rate equation describing this process is given in the Appendix [Eq. (5)]. The efflux induced is shown to be governed by the parameters for exit in the energized state. The quantity $\tilde{V}_{Si}^{T}$ is the maximum rate of exit of labeled AIB (S) into a medium containing a saturating concentration of unlabeled AIB (T), and $\tilde{K}_{Si}^{T}$ is the half-saturation constant for this process.

In the case of metabolic inhibitors, however, the efflux induced (Figs. 4A, 4B, 6A, 6B) is the direct result of de-energization and, as shown in the Appendix [Eq. (6)], it depends on the exit parameters in the de-energized state. The quantity $\overline{V}_{Si}^{*}$ is the maximum rate of exit into a medium where the concentration of S is negligible, and $\overline{K}_{Si}^{*}$ is the apparent affinity for this process. The asterisk distinguishes these parameters from the corresponding ones in the energized state. We have found that the efflux induced under these two different experimental conditions is virtually the same (Figs. 4A, 4B) and thus that according to Eq. (5) and (6):

$$\frac{\tilde{V}_{Si}^{T}}{1 + \tilde{K}_{Si}^{T}/[S_i]} = \frac{\overline{V}_{Si}^{*}}{1 + \overline{K}_{Si}^{*}/[S_i]}$$

This equality would be fulfilled if $\tilde{V}_{Si}^{T} = \overline{V}_{Si}^{*}$ and $\tilde{K}_{Si}^{T} = \overline{K}_{Si}^{*}$.

The effect of metabolic inhibitors such as DNP, CCCP, cyanide, or arsenate on the rate of entry (Figs. 5A, 5B) provides further evidence in support of the proposition that the energized step is the entry process. If accumulation were the result of a difference in the half-saturation constants inside and outside the cell and the energy were decreasing the affinity of the carrier for its substrate at the inner membrane surface, the rate of penetration of substrate into the cell should be relatively little affected by de-energization. This is indeed the case in the lactose transport system in *E. coli* [5, 11]. On the contrary, the effect of metabolic inhibitors on the entry rate of AIB in *M. phlei* is striking (Figs. 5A, 5B). Moreover, if the mechanism of energization in *M. phlei* were of the same nature as that demonstrated in the lactose transport system of *E. coli*, exchange of external labeled AIB with the amino

acids present in the pool would probably have produced a transient apparent accumulation of label or counterflow even in the de-energized state [9]; this, however, was not observed. It is therefore clear that the role of energy coupling in the active transport of AIB is to facilitate the entrance of substrate into the cell.

Although further discussion at this stage may be premature and speculative, it might prove useful in providing a working hypothesis for further experimentation. Our experiments have shown that the target for energy input is the entry process. The question arises as to whether this reflects a change in the maximum rate of entry or in the affinity of the carrier for the substrate at the external surface or both. One way of addressing this question is by comparing the magnitudes of the entry and exit rates in the energized state.

It was observed that cells which could maintain a concentration gradient of 11.800 exhibited a maximum rate of entry of approximately 0.57 nmoles/min · mg protein. The efflux induced by AIB in these same cells, containing 7.17 nmoles AIB/mg protein, was found to be 0.04 nmoles/min · mg protein and thus the two rates differed by a factor of approximately 13. Since a concentration of 1.03 mM AIB has not been shown to be saturating in the inside, it is possible for the maximum rate of exit to be higher than the observed rate, which would bring the two maximum rates (entry and exit) closer together. If on the contrary the amino acids inside the cell were indeed saturating, the specific activity of the AIB in the exit experiment would probably be approximately 1/4 of that in the entry experiment, due to competition by the internal pool, and the rate of exit would again have been underestimated. Thus, it would appear that the rates of entry and exit are approximately of the same magnitude. Even if these assumptions are inaccurate, a 13-fold difference in the maximum rates of transport in either direction cannot account for a concentration gradient of $1.18 \cdot 10^4$-fold.

If it is assumed therefore that in the energized state the rates of entry and exit do not differ significantly, the concentration gradient observed must be mainly the result of a difference in the dissociation constants ($\overline{V}_{Si} \approx \overline{V}_{So}$, $\overline{K}_{Si} > \overline{K}_{So}$). The simplest solution therefore would be to assume that the system in the de-energized state is completely symmetrical, $\overline{V}^*_{Si} = \overline{V}^*_{So}$ and $\overline{K}^*_{Si} = \overline{K}^*_{So}$, and that the energy increases the affinity of the carrier for the substrate in the external membrane surface.

This is not, however, the only possibility and, in fact, many studies in recent years have shown that facilitated transport systems which do not accumulate often exhibit extreme asymmetry in their specificity on the two membrane faces [12–14]. The possibility therefore that the system in the de-energized state is asymmetric so that $\overline{V}^*_{Si} > \overline{V}^*_{So}$, $\overline{K}^*_{Si} > \overline{K}^*_{So}$ and that the energy exerts its effect by increasing $\overline{V}^*_{So}$ to a magnitude comparable to that

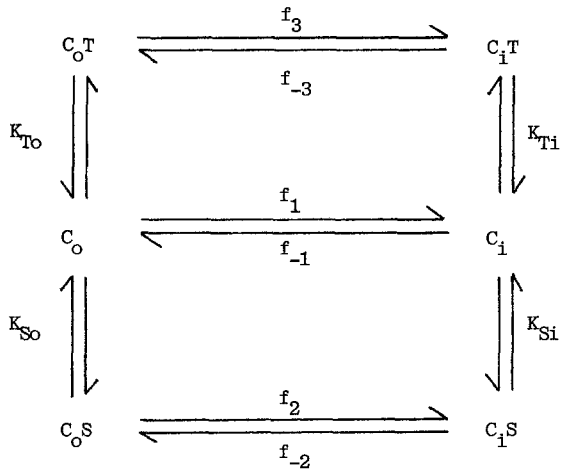

Fig. 7. Transport scheme for two substrates, S and T. Subscripts o and i refer to carrier forms on the outer and inner surfaces of the membrane, respectively; $f \pm i$ are rate constants for reorientation of carrier in the membrane. K_{So}, K_{To} are the equilibrium constants for carrier–substrate complex formation on the external surface for substrates S and T respectively, and K_{Si}, K_{Ti} the corresponding parameters on the inside.

of $\overline{V}^*_{Si}$ must be considered. It is important to note that the end result in both situations discussed is the same, but the mechanism of energization differs.

A simple change in $\overline{K}_{So}$ is in agreement with the experiments presented in this paper, but it does not explain a preliminary observation which showed

Table IV. Experimental Parameters Expressed in Terms of Individual Rate Constants for the Transport Scheme in Fig. 7[a]

Experimental parameter	Experiment	Labeled substrate	Unlabeled analog	Expression
$\overline{K}_{SI}$	zero *trans* exit	S_i	—	$K_{Si}\dfrac{(f_1+f_{-1})}{(f_1+f_{-2})}$
$\tilde{K}^T_{Si}$	infinite *trans* exit	S_i	T_0	$K_{Si}\dfrac{(f_{-1}+f_3)}{(f_{-2}+f_3)}$
$\overline{V}_{Si}$	zero *trans* exit	S_i	—	$\dfrac{f_1 f_{-2} C_t}{(f_1+f_{-2})}$
$\tilde{V}^T_{Si}$	infinite *trans* exit	S_i	T_0	$\dfrac{f_{-2} f_3 C_t}{(f_3+f_{-2})}$
$\overline{V}_{So}$	zero *trans* entry	S_0	—	$\dfrac{f_{-1} f_2 C_t}{(f_{-1}+f_2)}$

[a]The expressions shown in the table [15] have been derived under the assumption of rapid equilibrium. The quantity C_t represents the total concentration of the carrier in the membrane.

that partial inhibition of the rate of entry by CCCP cannot be overcome by raising the substrate concentration. This should occur if only $\overline{K}_{So}$ were affected by the energy. The second possibility is in agreement with our experiments provided the rate of entry is limited in the de-energized state by the return of the unloaded carrier to the external surface (f_{-1}) (see Fig. 7 and Table IV) and that the energy is put into the system to accelerate this step. The translocation of the carrier–substrate complex (f_2), which is the other process that determines the maximum rate of entry (Fig. 7, Table IV), cannot be rate limiting in the de-energized state because when cyanide and AIB were added together at the final steady state the efflux induced (a function of $\tilde{V}^{T}_{Si}{}^{*}$) was the same as when cyanide alone was added. An inspection of Table IV shows that if translocation of the carrier–substrate complex (f_2, f_3) were rate limiting, external AIB would have caused inhibition of the efflux induced by CN^-.

Appendix

General Rate Equation for the Transport of One Substrate in the Presence of Another

The rate of transport of substrate S in the presence of a second substrate T as derived by Devés and Krupka [15] is given as:

$$\frac{-d[S_i]}{dt} = \frac{\frac{\overline{V}_{Si}}{\overline{K}_{Si}}([S_i] - \alpha[S_o]) + \frac{\tilde{V}^{T}_{Si}}{\tilde{K}^{S}_{To}\overline{K}_{Si}}([S_i][T_o] - \frac{\alpha}{\beta}[S_o][T_i])}{1 + \frac{[S_o]}{\overline{K}_{So}} + \frac{[S_i]}{\overline{K}_{Si}} + \frac{[T_o]}{\overline{K}_{To}} + \frac{[T_i]}{\overline{K}_{Ti}} + \frac{[S_o][S_i]}{\tilde{K}^{S}_{So}\overline{K}_{Si}} + \frac{[T_o][T_i]}{\tilde{K}^{T}_{To}\overline{K}_{Ti}} + \frac{[S_o][T_i]}{\tilde{K}^{T}_{So}\overline{K}_{Ti}} + \frac{[T_o][S_i]}{\tilde{K}^{S}_{So}\overline{K}_{Si}}} \tag{3}$$

$[S_o]$ and $[T_o]$ represent the concentrations of substrates S and T outside the cell and $[S_i]$ and $[T_i]$ their concentration inside. The constants α and β are the ratios of the substrate concentrations inside and outside the cell after the final steady state has been achieved:

$$\alpha = \left(\frac{[S_i]}{[S_o]}\right)_{final} = \frac{\overline{V}_{So}\overline{K}_{Si}}{\overline{V}_{Si}\overline{K}_{So}}$$

$$\beta = \left(\frac{[T_i]}{[T_o]}\right)_{final} = \frac{\overline{V}_{To}\overline{K}_{Ti}}{\overline{V}_{Ti}\overline{K}_{To}}$$

All other constants are experimental parameters and their definitions are as follows:

$\overline{K}_{So}$, $\overline{K}_{To}$: half-saturation constants determined in zero *trans* experiments for S and T, respectively. The substrate undergoing transport is present outside the cell (o).

$\overline{K}_{Si}$, $\overline{K}_{Ti}$: constants determined in zero *trans* entry experiments for S and T, respectively. The substrate undergoing transport is present inside the cell (i).

$\tilde{K}^{S}_{So}$, $\tilde{K}^{T}_{To}$: constants determined in infinite *trans* entry experiments, for S and T, respectively. In each case the same substrate whose entry is followed is present on the *trans* side of the membrane at a saturating concentration.

$\tilde{K}^{T}_{So}$, $\tilde{K}^{S}_{To}$: constants determined in infinite *trans* entry experiments for the movement of S across the membrane into a solution containing T at a saturating concentration, and for the movement of T into saturating S, respectively.

$\overline{V}_{Si}$: maximum rate of zero *trans* exit of substrate S. The substrate undergoing transport is present inside the cell (i).

$\tilde{V}^{T}_{Si}$: maximum rate of infinite *trans* exit of substrate S into a solution of substrate T at a saturating concentration.

The equivalent expressions for some of the experimental parameters in Eq. (3) in terms of the rate constants in the scheme in Fig. 7 are shown in Table IV.

Rate Equation for the Efflux Induced by an Unlabeled Substrate Added at the Final Steady State

If T represents the unlabeled substrate and S the radioactive AIB, we find that under these experimental conditions $[T_o]/\overline{K}_{To} \gg [S_o]/\overline{K}_{So}$ and $[T_i] = 0$. Equation (3) thus simplifies to

$$\frac{-d[S_i]}{dt} = \frac{\tilde{V}^{T}_{Si}}{\overline{K}_{Si}\tilde{K}^{S}_{To}/[S_i]\overline{K}_{To} + 1} \tag{4}$$

Since $\tilde{K}^{T}_{Si} \cdot \overline{K}_{To} = \overline{K}_{Si} \cdot \tilde{K}^{S}_{To}$ (see [15]), Eq. (4) becomes

$$\frac{-d[S_i]}{dt} = \frac{\tilde{V}^{T}_{Si}}{\tilde{K}^{T}_{Si}/[S_i] + 1} \tag{5}$$

Rate Equation for the Efflux Induced when a Metabolic Inhibitor Is Added to the Final Steady State

In the absence of substrate T ($[T_i] = [T_o] = 0$), substrate S reaches its final steady state when $[S_i] = \alpha[S_o]$ and $-d[S_i]/dt = 0$.

If a metabolic inhibitor is now added to the system, the value of α drastically diminishes and $[S_i] \gg \alpha[S_o]$. Under this assumption Eq. (3) can be readily simplified to the following expression[2]:

$$\frac{-d[S_i]}{dt} = \frac{\overline{V}^*_{Si}}{1 + \overline{K}^*_{Si}/[S_i]} \tag{6}$$

The asterisk identifies the experimental parameters as those determined in the de-energized state.

Derivation of the Expression Used to Calculate the Relative Half-Saturation Constants for the Analogs with Respect to That for AIB

a. The rate equation for the influx of S in the presence of an unlabeled analog T in the external medium can be obtained from Eq. (3) by assuming that $[T_i] = [S_i] = 0$:

$$v = \frac{\overline{V}_{So}[S_o]/\overline{K}_{So}}{1 + [S_o]/\overline{K}_{So} + [T_o]/\overline{K}_{To}} \tag{7}$$

b. In the absence of the analog T ($[T_o] = 0$), the rate of entry is given by

$$v_o = \frac{\overline{V}_{So}[S_o]/\overline{K}_{So}}{1 + [S_o]/\overline{K}_{So}} \tag{8}$$

Dividing Eq. (8) by Eq. (7) we obtain

$$\left(\frac{v_o}{v} - 1\right) = \frac{[T_o]/\overline{K}_{To}}{1 + [S_o]/\overline{K}_{So}} \tag{9}$$

which when solved for $\overline{K}_{To}/\overline{K}_{So}$ becomes Eq. (2) in the Results section.

Acknowledgments

We would like to express our appreciation to Dr. F. S. Markland, Department of Biochemistry, University of Southern California, for carrying

[2]Equation (6) has been simplified assuming $\overline{K}_{So}/[S_o] \ll 1$ since under the present experimental conditions the value of this ratio, at the final steady state, is approximately 0.05.

out the amino acid analysis, and Miss Carol Papp for her expert secretarial assistance. This work was supported in part by an NIH Grant (AI-05637-17) and a U.S. Public Health Service International Fellowship to R.D. (TW002822).

References

1. A. A. Eddy, *Curr. Top. Membr. Transp.*, **10** (1978) 280–360.
2. D. B. Wilson, *Annu. Rev. Biochem.*, **47** (1978) 933–965.
3. F. M. Harold, *Curr. Top. Bioenerg.*, **6** (1977) 83–149.
4. R. Prasad, V. K. Kalra, and A. F. Brodie, *J. Biol. Chem.*, **251** (1976) 2493–2497.
5. H. H. Winkler and T. H. Wilson, *J. Biol. Chem.*, **241** (1966) 2200–2211.
6. D. H. Spackman, W. H. Stein, and S. Moore, *Anal. Chem.*, **30** (1958) 1190–1206.
7. O. H. Lowry, N. J. Rosebrough, A. L. Farr, and R. J. Randall, *J. Biol. Chem.*, **193** (1951) 265–275.
8. R. Devés and R. M. Krupka, *Biochim. Biophys. Acta*, **556** (1979) 533–547.
9. P. T. S. Wong, E. R. Kashket, and T. H. Wilson, *Proc. Natl. Acad. Sci. U.S.A.*, **65** (1970) 63–69.
10. J. R. Lancaster and P. C. Hinkle, *J. Biol. Chem.*, **252** (1970) 7657–7661.
11. M. J. Osborn, W. L. McLellan, and B. L. Horecker, *J. Biol. Chem.*, **236** (1961) 2585–2589.
12. G. F. Baker and W. F. Widdas, *J. Physiol.*, **231** (1973) 143–165.
13. J. E. G. Barnett, G. D. Holman, R. A. Chalkley, and K. A. Munday, *Biochem. J.*, **145** (1975) 417–429.
14. M. Klingenberg, H. Aguila, R. Kramer, W. Babel, and J. Feckl, in *Biochemistry of Membrane Transport*, FEBS-Symposium No. 42 (G. Semenza and E. Carafoli, eds.), Springer-Verlag, New York (1977), pp. 567–579.
15. R. Devés and R. M. Krupka, *Biochim. Biophys. Acta*, **556** (1979) 533–547.